Materials and Design 81 (2015) 31–38

Contents lists available at ScienceDirect

Materials and Design

journal homepage: www.elsevier.com/locate/matdes

Effects of nano-particles strengthening activating flux on the microstructures and mechanical properties of TIG welded AZ31 magnesium alloy joints

Xiong Xie, Jun Shen *, Liang Cheng, Yang Li, Yayun Pu

State Key Laboratory of Mechanical Transmission, College of Materials Science and Engineering, Chongqing University, Chongqing 400044, People's Republic of China

A R T I C L E I N F O

Article history:
Received 6 January 2015
Revised 6 May 2015
Accepted 9 May 2015
Available online 11 May 2015

Keywords:
AZ31 magnesium alloy
Tungsten inert gas welding
Nano-particles strengthening activating flux
Surface coating density
Macro-appearance
Microstructure
Mechanical properties

A B S T R A C T

In this paper, AZ31 magnesium alloy joints were processed by nano-particles strengthening activating flux tungsten inert gas (NSA-TIG) welding, which was achieved by the mixed TiO_2 and nano-SiC particles coated on the samples before welding tests. The macro/micro structural observation and mechanical properties evaluation of the welding joints were conducted by using optical microscope, scanning electron microscope, energy dispersive X-ray spectroscopy, X-ray diffraction and tension and microhardness tests. The results showed that nano-particles strengthening activating flux effective improved the microstructure, microhardness in fusion zone, ultimate tensile strength of the TIG welding joints. In addition, the chemical reaction between part of SiC particles and AZ31 magnesium alloy produced Al_4C_3 and Mg_2Si in the joints. The Al_4C_3 performed as nucleating agents for α-Mg and the dispersed Mg_2Si and SiC particles enhanced the mechanical properties of the NSA-TIG welding joints. However, large heat input induced by the increase of the surface coating density of the nano-particles strengthening activating flux, increased the α-Mg grain sizes and weakened the mechanical properties of the welded joints. Therefore, the grain size of α-Mg, distribution of β-$Mg_{17}Al_{12}$, Mg_2Si and SiC particles together influenced the evolution of the mechanical properties of the NSA-TIG welded AZ31 magnesium alloy joints.

1. Introduction

Recently, there has been an increasing demand for light weight and high specific strength materials in the automotive industry because of resource and environmental concerns [1,2]. Magnesium (Mg) alloys have been receiving a considerable interest in this regard since Mg is approximately 75% and 34% lighter than steel and aluminum, respectively [3,4]. Therefore, high-quality welding techniques are required for the manufacture of complex Mg alloy structures. Because of its practicability and economy, tungsten inert gas (TIG) [5,6] welding is used more widely for the manufacture of Mg alloy components compared with laser beam welding (LBW) [7], electron beam welding (EBW) [8] and friction stir welding (FSW) [9] and ultrasonic spot welding (USW) [10]. However, one problem in the TIG welding of magnesium alloys is the shallow penetration. Improving heat input would increase penetration while the grains in the joints are coarse when heat input is high [11].

A novel technique, which is named as activating flux tungsten inert gas (A-TIG) welding, was invented by Paton Welding Institute for this problem. In this technique, the penetration was deepened by the arc constriction and reversed Marangoni convection induced by the activating flux coated on the surface of weldments prior to welding process [12,13]. On this basis, various types of activating fluxes were developed and their effects on the microstructures and mechanical properties of TIG welded magnesium alloys joints were studied. Chen et al. [14], Shen et al. [15] and Liu et al. [16,17] studied the effects of activating fluxes (CaF_2, MgO, CaO, TiO_2, MnO_2, Cr_2O_3 and $MnCl_2$) on the A-TIG welded joints, respectively. All of these activating fluxes improved the penetration apparently. However, it was found that the overgrowth of grains in the joints cannot be avoided completely because the activating fluxes prevented the heating radiation of welding pool during the welding process, although the welding penetration increased.

To solve this problem, SiC particles were added in the activating fluxes by Liu and Sun [18] because of their good wettability for magnesium and their roles as nucleation agents for α-Mg grains and obstacles against the grains growth during the solidification of welding pool, which was named as SiC particles strengthening

---

* Corresponding author.
E-mail address: shenjun@cqu.edu.cn (J. Shen).

http://dx.doi.org/10.1016/j.matdes.2015.05.024
0261-3069/

activating flux tungsten inert gas (SA-TIG) welding technique. As the effective improvement of mechanical properties of Mg alloys joints induced by the SA-TIG welding technique, Shen et al. [19,20] refined the size of SiC particles from micrometers to nanometers further. Compared with the SA-TIG welding joints, the joints welded by nano-sized SiC particles strengthening activating flux tungsten inert gas (NSA-TIG) welding had a higher quality of microstructure and mechanical properties.

Since the influence of activating flux densities on the microstructures and mechanical properties of NSA-TIG welded magnesium alloys joints was still unclear, different surface coating density of the nano-particles strengthening activating (NSA) fluxes were applied in the NSA-TIG welding tests of AZ31 magnesium alloy plates and their effects were discussed in details.

2. Experimental procedures

Six groups of commercial hot-extruded AZ31 magnesium alloy plates with a size of 150 mm × 100 mm × 5 mm were used for the NSA-TIG welding tests. Its chemical compositions and mechanical properties are listed in Table 1. For each welding condition, at least five specimens were produced. Two of these were used for metallographic examination. The other three were tensile shear test specimens. NSA flux was the mixed TiO_2 powder (48 μm, 60 wt.%) and SiC particles (40 nm, 40 wt.%) by absolute ethyl alcohol. A brush was used to apply it evenly to the top surface of each specimen with a width of 10 mm. The mass of plates before coating (m_1) and the mass of plates after coating (m_2) were weighted using an electrical analytical balance (with accuracy of 1 mg). Then, the amounts of the flux coating on the unit area of different specimens ρ_A were calculated by the formula as follows:

$$\rho_A = \frac{m_2 - m_1}{S} \tag{1}$$

where S is the coated area. The surface coating densities of the NSA flux were (a) 0 mg/cm^2, (b) 5.00 ± 0.32 mg/cm^2, (c) 10.00 ± 0.15 mg/cm^2, (d) 15.00 ± 0.34 mg/cm^2, (e) 20.00 ± 0.23 mg/cm^2 and (f) 30 ± 0.19 mg/cm^2. Ahead of coating activating flux, the top surface of each specimen was grounded using a grinder and then cleaned with acetone to remove oxides and grease. Then, an AC automatic welding machine (NSA-500-1) with an arc voltage control (HAS-01-A) was adopted for butt-welding. The detailed welded parameters in these experiments were: welding voltage was 80 A, welding speed was 60 mm/min, electrode distance was 2 mm and flow rate of argon gas was 7.5 L/min, and all these parameter are constant.

Table 1
Chemical composition of AZ31 magnesium alloy (wt.%).

Mg	Al	Zn	Mn	Si	Cu	Ca	Fe	Ni
95.37	3.27	0.91	0.25	0.10	0.05	0.04	0.005	0.005

After the welding tests, the welded seam surfaces were photographed by camera, and the samples were sectioned and the cross-sections of the welded pools were prepared by using standard metallographic procedures (grinding, polishing and etching with a solution of 1 g picric acid + 10 mL ethyl alcohol + 2 mL acetic acid + 2 mL distilled water). An optical microscopy (MDJ200) and a scanning electron microscope (SEM, TESCAN 95 VEGA IILMV) were applied to observe the cross-sectional macrographs, the fracture surface and the microstructures of the welded joints. The phases in the NSA-TIG welded AZ31 magnesium alloy joints were analyzed by the Energy dispersive X-ray spectroscopy (EDS, OXFORD, ISIS300) and the X-ray diffraction (XRD, D/Max-2500PC, made by Rigaku Corporation, Japan) operated with an incident beam with a 300 mm diameter using Cu Kα radiation (wave length λ = 0.15406 nm) at 45 kV and 40 mA, and a sample tilt ψ angle ranging from 10° to 90° with a step size of 5° and 3 s in each step. In addition, the microhardness tests were performed with a Vickers hardness tester (HX-1000 TM) with a period of 15 s, a load of 50 g and a step size of 0.5 mm. The values of the microhardness of the heat affected zone (HAZ) and fusion zone (FZ) were made from an average value of five data points. In order to avoid the influence of the BM (the welding joint is a partial penetration bead), only the melted parts of the joints were machined into tensile specimens. Two types of tensile test specimens were machined with ASTM standard: E8/E8M – 13a, transverse specimens containing the welding joints in the center of the gauge length (AT) and basic materials (BT) (as seen in Fig. 1). The tensile tests were carried out with an electronic tensile test machine (SANS XYA105C) at room temperature with a rate of 1 mm/min. Three tensile test results were collected in samples with the same surface coating density of the NSA flux and the average values of them were adopted for discussion.

3. Results and discussion

3.1. Effects of surface coating density of the NSA flux on macro appearances of NSA-TIG welded AZ31 magnesium alloy seams

The images of welding seams surface appearances and the outlines of the FZ of the NSA-TIG welded joints at different surface coating density of the NSA fluxes are showed in Figs. 2 and 3.

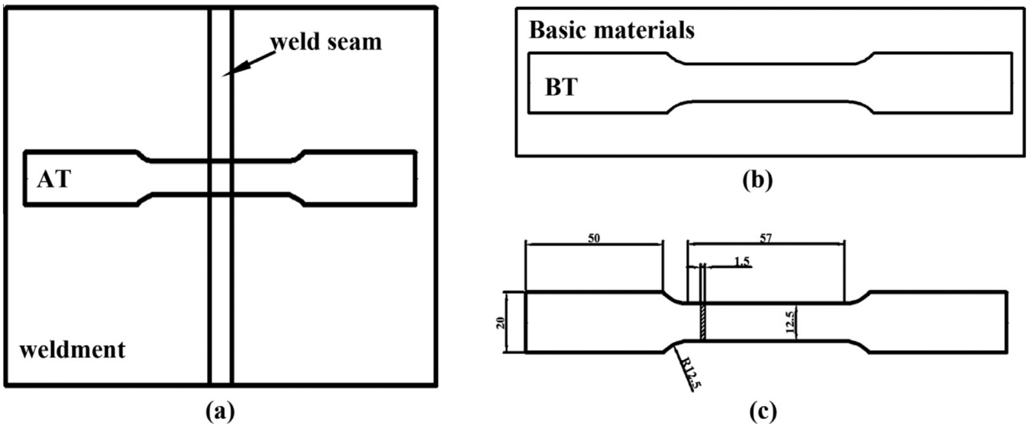

Fig. 1. Schematic drawing of tensile test specimens: (a) positions of AT tensile specimens in the weldments; (b) positions of BT tensile specimens in the basic materials and (c) dimension of tensile specimens in mm.